Detecting sugarcane 'orange rust' disease using EO-1 Hyperion hyperspectral imagery

A. APAN
Geospatial Information and Remote Sensing (GIRS) Group, Faculty of Engineering and Surveying, University of Southern Queensland, Toowoomba 4350 QLD, Australia; e-mail: apana@usq.edu.au

A. HELD
Environmental Remote Sensing Group, CSIRO Land and Water, PO Box 1666, Canberra, ACT 2601 Australia

S. PHINN
Biophysical Remote Sensing Group, School of Geography, Planning & Architecture, University of Queensland, Brisbane 4072, Australia

J. MARKLEY
Mackay Sugar, Post Office Pleystowe, Pleystowe 4741 QLD, Australia

Abstract
This Letter evaluates several narrow-band indices from EO-1 Hyperion imagery in discriminating sugarcane areas affected by 'orange rust' (Puccinia kuehnii) disease. Forty spectral vegetation indices (SVIs), focusing on bands related to leaf pigments, leaf internal structure, and leaf water content, were generated from an image acquired over Mackay, Queensland, Australia. Discriminant function analysis was used to select an optimum set of indices based on their correlations with the discriminant function. The predictive ability of each index was also assessed based on the accuracy of classification. Results demonstrated that Hyperion imagery can be used to detect orange rust disease in sugarcane crops. While some indices that only used visible near-infrared (VNIR) bands (e.g. SIPI and R800/R680) offer separability, the combination of VNIR bands with the moisture-sensitive band (1660 nm) yielded increased separability of rust-affected areas. The newly formulated 'Disease–Water Stress Indices' (DWSI-1~R800/R1660; DSWI-2~R1660/R550; DWSI-5~(R800zR550)/ (R1660zR680)) produced the largest correlations, indicating their superior ability to discriminate sugarcane areas affected by orange rust disease.

1. Introduction
Disease management is important in maintaining the competitive advantage of the Australian sugar industry (Croft et al. 2000). Pathogens can cause serious damage to sugarcane (Saccharum spp.) crops that often lead to reduced crop yield and quality. Dealing with this problem involves a variety of curative measures, where disease detection and mapping play a central role. For instance, to apply chemicals for disease control, the location and spatial extent of affected crops must be first determined.

Although the use of airborne and satellite remotely sensed data in detecting crop diseases and in situ assessment of crop quality is not new (e.g. Kanemasu et al. 1974), no scientific literature have been found on hyperspectral data processing to map sugarcane disease. However, extensive work has been completed, successfully demonstrating the use of narrow-band spectral indices for general assessment of crop condition (Thenkabail et al. 2002). Therefore, the aim of the study was to examine the

potential of satellite hyperspectral imagery to detect the incidence of sugarcane 'orange rust' disease. The specific objectives were:
(a) to test the utility of existing spectral vegetation indices (SVIs);
(b) to develop indices relevant to disease detection; and
(c) to gain insights on the relationship between sugarcane orange rust disease and changes to the biochemical component of the crop.

2. Research methods

2.1. Study area, Hyperion data and pre-processing

The study area is approximately centred at 149‡4' E and 21‡15' S and covers a portion of Mackay's sugarcane growing region in Queensland (figure 1). This is the largest sugar-producing area in Australia.

An image from the Hyperion sensor on EO-1 was acquired on 2 April 2002, and delivered as Level 1B_1 data in scaled radiance units. To facilitate the development of indices, these values were converted to apparent surface reflectance using ACORN 4.10 software (Analytical Imaging and Geophysics LLC 2002). Prior to this conversion, the following pre-processing steps were implemented: re-calibration, band selection, de-streaking, and repair of 'bad' (non-responsive) pixel values

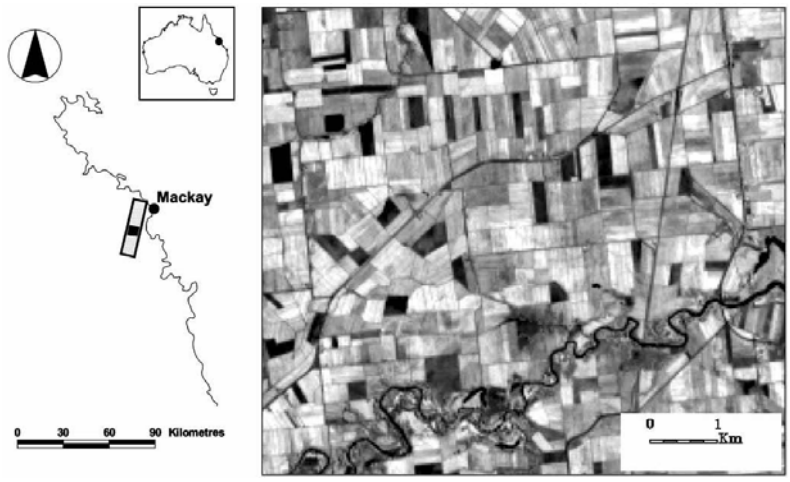

Figure 1. Greyscale Hyperion image subset (800 nm) captured over a section of the Mackay sugarcane region on 2 April 2002.

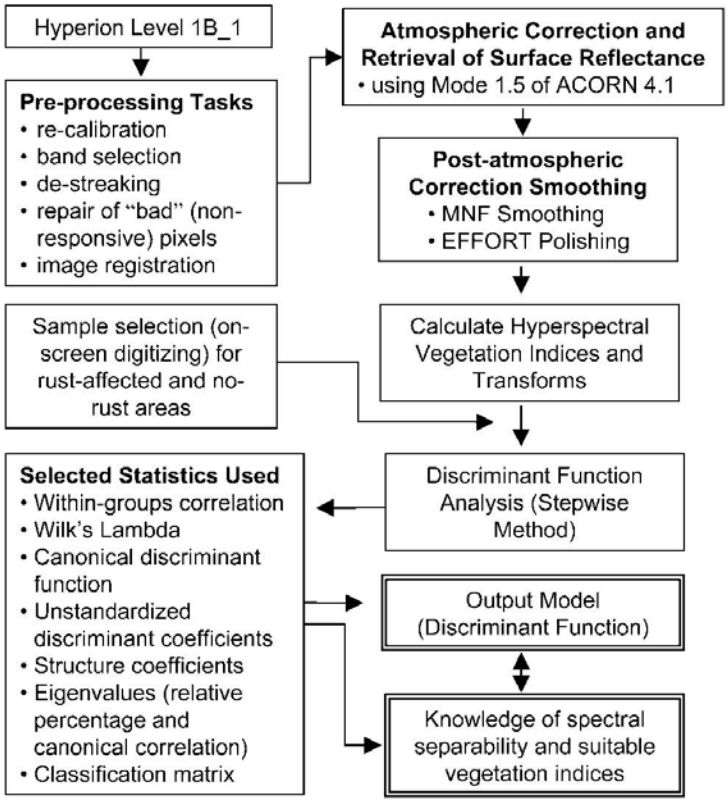

Figure 2. Major steps in the processing of the Hyperion image for the spectral discrimination of sugarcane orange rust in this study.

(figure 2) (Apan and Held 2002; Datt et al., 2003). A minimum noise fraction (MNF) transformation smoothing was applied to the post-atmospheric correction reflectance image to minimize uncorrelated spatial noise. The output image was further processed by applying the Empirical Flat Field Optimal Reflectance Transformation (EFFORT) polishing technique (Boardman 1998).

2.2. Sugarcane disease and generation of relevant hyperspectral indices

Orange rust is a fungal disease in sugarcane that produces orange leaf lesions (pustules) and tend to be grouped in patches. The ruptured leaves allow water to escape from the plant, leading to moisture stress (Croft et al. 2000). Orange rust occurs in summer/autumn and is favoured by humid warm conditions. In this study, the infected fields were rated at the canopy level as '4', based on our 1–5 scale (1 has lowest severity to 5 with highest severity). Referenced at the time of Hyperion overpass on 2 April 2002, the information on the location and severity rating of orange rust was sourced from field officers of Mackay Sugar co-operative.

Diagnostic symptoms of orange rust in image datasets may be related to changes in leaf pigments, internal leaf structure, and moisture content. Thus, SVIs focusing on one

or more attributes associated with these symptoms were selected (table 1). The majority of indices were sourced from the literature, while five indices were formulated in this study based from the examination of detailed spectral reflectance plots.

Table 1. Vegetation indices used in this study.

Name	Formula*	References
1. Simple Ratio (SR) 750/705	R750/R705	Gitelson and Merzlyak 1994
2. SR 800/550	R800/R550	
3. Normalized Difference (ND) 750/660	(R750−660)/(R750+R660)	
4. ND 800/680	(R800−R680)/(R800+R680)	Sims and Gamon 2002
5. ND 750/705	(R750−R705)/(R750+R705)	Gitelson and Merzlyak 1994
6. Modified SR (MSR) 705/445	(R750−R445)/(R705−R445)	Sims and Gamon 2002
7. Modified ND (MND) 750/705	(R750−R445)/(R750+R705−2R445)	Sims and Gamon 2002
8. SR 750/550	R750/R550	Gitelson and Merzlyak 1994
9. Chlorophyll Well (Chloro-well)	algorithm to derive certain value between R550 and R760	CSIRO VegSpectra†
10. Green Peak Well (Green-well)	algorithm to derive certain value between R500 and R680	CSIRO VegSpectra†
11. Ave(750–850)	average between R750 and R850	
12. Modified Chlorophyll Absorption in Reflectance Index (MCARI)	[(R700−R670)–0.2(R700−R550)] (R700/R670)	Daughtry *et al.* 2000
13. Transformed Chlorophyll Absorption in Reflectance Index (TCARI)	3[(R700−R670)–0.2(R700−R550) (R700/R670)]	Haboudane *et al.* 2002
14. Optimized Soil-Adjusted Vegetation Index (OSAVI)	(1+0.16)(R800−R670)/(R800+R670+0.16)	Rondeaux *et al.* 1996
15. Ratio TCARI/OSAVI	TCARI/OSAVI	Haboudane *et al.* 2002
16. Plant Senescence Reflectance Index (PSRI)	(R680−R500)/R750	Merzlyak *et al.* 1999
17. Structure-Insensitive Pigment Index (SIPI)	(R800−R445)/(R800−R680)	Peñuelas *et al.* 1995
18. Photochemical Reflectance Index (PRI)	(R531−R570)/(R531+R570)	Gamon *et al.* 1992
19. Pigment Specific SR (chlorophyll a) (PSSRa)	R800/R680	Blackburn 1998
20. PSSR (chlorophyll b) (PSSRb)	R800/R635	Blackburn 1998
21. SR 695/420	R695/R420	Carter 1994
22. SR 695/760	R695/R760	Carter 1994
23. Red Edge Inflection Point (Lagrangian model) (REIP-Lagr)	first derivative of R690, R733, and R752; then apply formula	Dawson and Curran 1998

Table 1. (*Continued*)

Name	Formula*	References
24. Red Edge Inflection Point (polynomial model) (REIP-poly)	second derivative of R690 and R750; then apply formula	Broge and Leblanc 2001
25. Principal component 1 (PC1)	principal component transform	
26. Principal component 2 (PC2)	principal component transform	
27. Disease–Water Stress Index 1 (DSWI-1)	R800/R1660	this study
28. DSWI-2	R1660/R550	this study
29. DSWI-3	R1660/R680	this study
30. DSWI-4	R550/R680	this study
31. DSWI-5	(R800+R550)/(R1660+R680)	this study
32. NDWI-Hyperion (NDWI-Hyp)	(1070−1200)/(1070+1200)	Ustin *et al.* 2002
33. ND Water Index (NDWI)	(R860−R1240)/(R860+R1240)	Gao 1996
34. Water Index (WI)	R900/R970	Peñuelas *et al.* 1997
35. Ratio of WI and ND 750/660	WI/ND750	
36. Moisture Stress Index (MSI)	R1600/R820	Hunt and Rock 1989
37. Water Well 3PT (983) (WW 983)	apply 3PT formula (well near R983)	CSIRO VegSpectra†
38. Water Well 3PT (1205) (WW 1205)	apply 3PT formula (well near R1205)	CSIRO VegSpectra†
39. Ratio of WW 983 and PSSRa	WW 983/PSSRa	
40. Ratio of WW 1205 and PSSRa	WW 1205/PSSRa	

*R = reflectance.
†Unpublished.

2.3. Statistical analyses

Polygons were digitized around sugarcane blocks affected with the orange rust disease and several blocks not affected by the disease to produce 142 and 159 sample pixels, respectively. The non-diseased blocks contained the same variety (Q124) and age group of sugarcane as the diseased blocks. A discriminant function analysis was used to generate discriminant functions based on linear combinations of Hyperion band indices that provided optimum discrimination between rust affected and non-rust affected areas (SPSS 2001). The evaluation of the model's accuracy was performed by classifying a 'hold-out sample' (i.e. those pixels not included in model generation) corresponding to 30% of the total sample pixels.

3. Results and discussion

Reflectance spectra of Hyperion 'raw' bands show that sample areas with the sugarcane orange rust disease exhibit difference in spectral reflectance signatures and can be discriminated from non-diseased areas, at certain wavelengths (figure 3). The highest separability was located in the NIR region (between 750 to 880 nm and 1070 nm). This was followed by selected ranges in the short wave infrared (SWIR; 1660 nm and 2200 nm), green (550 nm) and red (680 nm) regions.

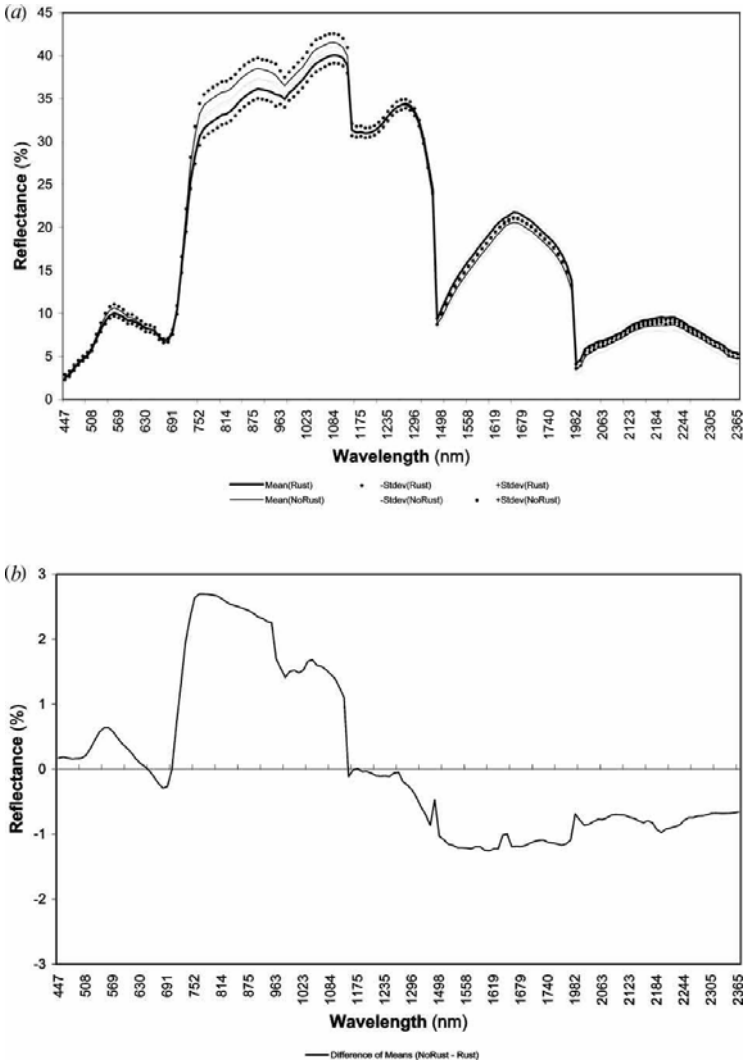

Figure 3. Reflectance spectra of Hyperion sample pixels containing sugarcane orange rust disease and without orange rust disease: (a) mean and standard deviations and (b) difference of means.

Disease-affected areas have relatively lower reflectance values than unaffected sites in the green and NIR regions. However, the reverse is true for the red and the SWIR domains, areas with orange rust have higher reflectance values than no-rust sugarcane.

The results of the discriminant function analysis (table 2) indicate the following.

Table 2. Selected statistics from the discriminant function analysis.

Index*	Structure coefficient†	Canonical correlation‡ and accuracy§	Index*	Structure coefficient†	Canonical correlation‡ and accuracy§
1. DWSI-1	−0.839	0.781 (94.9%)	21. ND750/705	−0.439	0.578 (75.5%)
2. DWSI-2	0.835	0.785 (92.9%)	22. SR750/705	−0.433	0.569 (75.5%)
3. DWSI-5	−0.811	0.781 (93.9%)	23. MCARI	−0.405	0.534 (77.6%)
4. MSI	0.803	0.765 (92.9%)	24. SR695/420	0.404	0.523 (83.7%)
5. NDWI_Hyp	−0.796	0.770 (94.9%)	25. PSSRb	−0.403	0.518 (73.5%)
6. NDWI	−0.749	0.780 (93.9%)	26. WW983	−0.361	0.493 (72.6%)
7. Ave(750–850)	−0.703	0.739 (87.8%)	27. WW1205/PSSRa	−0.358	0.379 (66.3%)
8. SIPI	0.629	0.698 (85.7%)	28. TCARI/OSAVI	−0.326	0.459 (69.4%)
9. WW1205	−0.627	0.649 (84.7%)	29. WI/ND750/660	0.309	0.355 (66.3%)
10. PC1	0.610	0.623 (90.8%)	30. SR750/550	−0.282	0.296 (65.3%)
11. PC2	−0.603	0.635 (82.7%)	31. PSRI	0.229	0.364 (65.3%)
12. DWSI-4	−0.563	0.709 (88.8%)	32. SR800/550	−0.227	0.238 (64.3%)
13. ND800/680	−0.508	0.632 (86.7%)	33. DSWI-3	0.166	0.121 (62.2%)
14. SR695/760	0.507	0.630 (84.7%)	34. WI	−0.150	0.350 (70.4%)
15. OSAVI	−0.496	0.617 (85.7%)	35. Green-well	0.126	0.116 (52.0%)
16. TCARI	−0.493	0.620 (79.6%)	36. PRI	0.094	0.041 (65.3%)
17. PSSRa	−0.493	0.632 (85.7%)	37. REIP-Lagr	−0.079	0.112 (59.2%)
18. ND750/660	−0.490	0.605 (83.7%)	38. Chloro-well	−0.077	0.025 (56.1%)
19. MND750/705	−0.477	0.603 (79.6%)	39. WW983/PSSRa	0.077	0.234 (56.1%)
20. MSR705/445	−0.474	0.590 (76.5%)	40. REIP-poly	−0.029	0.004 (48.0%)

*Variables ordered by absolute size of correlation within function.
†Pooled within-groups correlations between discriminating variables and standardized canonical discriminant function.
‡Single-variable run canonical correlation (interpretation is equivalent to Pearson correlation coefficient).
§Accuracy (per cent of cases correctly classified by the model) is based from 'hold-out sample' grouped cases.

- The 1600 nm (SWIR) band, if combined by ratioing with either NIR band (800 nm) or green band (550 nm), will produce the best (i.e. the largest correlation with the discriminant function and the highest classification accuracy) among the indices. This is the case for the four highest ranked indices (DWSI-1, DSWI-2, DSWI-5 and MSI).
- The indices that only incorporate selected bands in the VNIR (e.g. Ave(750–850, SIPI, DSWI-4, ND800/600, OSAVI, TCARI, PSSRa, etc.) performed moderately.
- The indices developed from the reflectance red-edge (690–720 nm) (e.g. REIP-Lagr and REIP-poly) were relatively poor in discriminating diseased from non-diseased sugarcane crops. They produced very small correlations with the discriminant function and their classification accuracies were among the lowest.

The output discriminant function, a linear combination of DSWI-2, SR695/420 and NDWI-Hyp, attained a classification accuracy of 96.9% for the hold-out sample pixels.

The results show that spectral discrimination of sugarcane with a moderate to high severity of orange rust disease in the Mackay region sampled by the Hyperion image could be significantly increased by incorporating moisture-sensitive bands in the SWIR region. The loss of moisture due to lesions or ruptured leaves plays an important factor in the disease detection (Croft et al. 2000). The high levels of discrimination provided by the selected Disease–Water Stress Indices developed from this study reinforce the point. However, water-stressed crops, but not necessarily afflicted with orange rust disease, could potentially be differentiated from these indices. Such conditions would complicate orange rust detection.

There is a need to assess if areas with low to moderate sugarcane orange rust infection (i.e. early to middle stages) will produce significantly different reflectance signatures from non-diseased areas. This will be the focus of the next phase of the study, and is considered relevant. Early disease detection is crucial to enable swift

deployment of curative and preventive measures. Thus, it is desirable to test the Hyperion image in early-stage disease detection. Under this condition, however, it is not known if moisture differentiation (hence using the SWIR bands) may be the most crucial factor to rely on.

4. Conclusions

Several narrow band indices derived from Hyperion image data were able to discriminate sugarcane crops severely affected by orange rust disease from non-diseased areas in the Mackay region of Australia. The indices developed used spectral bands that are known to be sensitive to changes in leaf pigments, internal leaf structure and moisture content. The discriminant function analysis allowed the 'ranking' of each index based on their ability to differentiate rust-affected from non rust-affected pixels. While the VNIR-based indices offer significant separability, the incorporation of a 1660 nm SWIR band that led to the formulation of the Disease– Water Stress Indices provided the maximum discrimination. The follow-on study on assessing Hyperion's ability to detect rust disease at various levels of severity will provide additional information on the use of hyperspectral sensors in crop protection.

Acknowledgments

We thank Guy Byrne and Alan Marks (CSIRO) for their help during the field work. The mathematical formulation of the DSWI-5 index was suggested by Peter Dunn (USQ). Bisun Datt (CSIRO) provided valuable advice during the preprocessing of Hyperion imagery.

References

ANALYTICAL IMAGING AND GEOPHYSICS LLC, 2002, ACORN Version 4.10 (Boulder, CO: AIG).

APAN, A., and HELD, A., 2002, In-House Workshop on Hyperion Data Processing: Echo-ing the Sugarcane Project Experience (Black Mountain Laboratories, Canberra: CSIRO Land and Water).

BLACKBURN, G. A., 1998, Spectral indices for estimating photosynthetic pigment concentrations: a test using senescent tree leaves. International Journal of Remote Sensing, 19, 657–675.

BOARDMAN, J. W., 1998, Post-ATREM polishing of AVIRIS apparent reflectance data using EFFORT: a lesson in accuracy versus precision. In Summaries of the Seventh JPL Airborne Earth Science Workshop (Pasadena, CA: JPL), Vol. 1, p. 53.

BROGE, N. H., and LEBLANC, E., 2001, Comparing prediction power and stability of broadband and hyperspectral vegetation indices for estimation of green leaf area index and canopy chlorophyll density. Remote Sensing of the Environment, 76, 156–172.

CARTER, G. A., 1994, Ratios of leaf reflectances in narrow wavebands as indicators of plant stress. International Journal of Remote Sensing, 15, 697–703.

CROFT, B., MAGAREY, R., and WHITTLE, P., 2000, Disease management. In Manual of Canegrowing, edited by M. Hogarth and P. Allsopp (Brisbane: Bureau of Sugar Experiment Stations), pp. 263–289.

DATT, B., MCVICAR, T. R., VAN NIEL, T. G., JUPP, D. L. B., and PEARLMAN, J. S., 2003, Pre-processing EO-1 Hyperion hyperspectral data to support the application of agricultural indexes. IEEE Transactions on Geoscience and Remote Sensing, 41, 1246– 1259.

DAUGHTRY, C. S. T., WALTHALL, C. L., KIM, M. S., BROWN DE COLSTOUN, E., and MCMURTREY III, J. E., 2000, Estimating corn leaf chlorophyll concentration from leaf and

canopy reflectance. Remote Sensing of Environment, 74, 229–239.
DAWSON, T. P., and CURRAN, P. J., 1998, A new technique for interpolating the reflectance red edge position. International Journal of Remote Sensing, 19, 2133–2139.
GAMON, J. A., PEN˜ EULAS, J., and FIELD, C. B., 1992, A narrow-waveband spectral index that tracks diurnal changes in photosynthetic efficiency. Remote Sensing of Environment, 41, 35–44.
GAO, B., 1996, NDWI—a normalized difference water index for remote sensing of vegetation liquid water from space. Remote Sensing of Environment, 58, 257–266.
GITELSON, A. A., and MERZLYAK, M. N., 1994, Spectral reflectance changes associate with autumn senescence of Aesculus hippocastanum L., and Acer platanoides L. leaves. Spectral features and relation to chlorophyll estimation. Journal of Plant Physiology, 143, 286–292.
HABOUDANE, D., MILLER, J. R., TREMBLAY, N., ZARCO-TEJADA, P. J., and DEXTRAZE, L., 2002, Integrated narrow-band vegetation indices for prediction of crop chlorophyll content for application to precision agriculture. Remote Sensing of Environment, 81, 416–426.
HUNT, E. R., and ROCK, B. N., 1989, Detection of changes in leaf water content using near-and middle-infrared reflectances. Remote Sensing of Environment, 30, 43–54.
KANEMASU, E. T., NIBLETT, C. L., MANGES, H., LENHERT, D., and NEWMAN, M. A., 1974, Wheat: its growth and disease severity as deduced from ERTS-1. Remote Sensing of Environment, 3, 255–260.
MERZLYAK, M. N., GITELSON, A. A., CHIVKUNOVA, O. B., and RAKITIN, V. Y., 1999, Nondestructive optical detection of pigment changes during leaf senescence and fruit ripening. Physiologica Plantarum, 106, 135–141.
PEN˜UELAS, J., BARET, F., and FILELLA, I., 1995, Semi-empirical indices to assess carotenoids/ chlorophyll a ratio from leaf spectral reflectance. Photosynthetica, 31, 221–230.
PEN˜UELAS, J., PINOL, R. O., OGAYA, R., and FILELLA, I., 1997, Estimation of plant water concentration by the reflectance Water Index WI (R900/R970). International Journal of Remote Sensing, 18, 2869–2875.
RONDEAUX, G., STEVEN, M., and BARET, F., 1996, Optimization of Soil-Adjusted Vegetation Indices. Remote Sensing of Environment, 55, 95–107.
SIMS, D. A., and GAMON, J. A., 2002, Relationship between leaf pigment content and spectral reflectance across a wide range of species, leaf structures and developmental stages. Remote Sensing of Environment, 81, 337–354.
SPSS, 2001, SPSS for Windows (Release 11) (Chicago: SPSS).
THENKABAIL, P., SMITH, R., and DEPAUW, E., 2002, Evaluation of narrowband and broadband vegetation indices for determining optimal hyperspectral wavebands for agricultural crop characterisation. Photogrammetric Engineering and Remote Sensing, 68, 607–621.
USTIN, S. L., ROBERTS, D. A., GARDNER, M., and DENNISON, P., 2002, Evaluation of the potential of Hyperion data to estimate wildfire hazard in the Santa Ynez Front Range, Santa Barbara, California. Proceedings of the 2002 IEEE IGARSS and 24th Canadian Symposium on Remote Sensing, Toronto, Canada, 24–28 June 2002 (Piscataway, NJ: IEEE), pp. 796–798.